Thermally reduced graphenes exhibiting a close relationship to amorphous carbon

Wong, Colin Hong An; Ambrosi, Adriano; Pumera, Martin

2012

Wong, C. H. A., Ambrosi, A., & Pumera, M. (2012). Thermally Reduced Graphenes Exhibiting a Close Relationship to Amorphous Carbon. Nanoscale, 4(16), 4972-4977.

https://hdl.handle.net/10356/95873

https://doi.org/10.1039/C2NR30989K

Nanoscale

Dynamic Article Links ►

Cite this: DOI: 10.1039/c0xx00000x

www.rsc.org/xxxxxx

ARTICLE TYPE

Thermally reduced graphenes exhibiting a close relationship to amorphous carbon

Colin Hong An Wong, Adriano Ambrosi and Martin Pumera*

Received (in XXX, XXX) Xth XXXXXXXXX 20XX, Accepted Xth XXXXXXXXX 20XX
DOI: 10.1039/b000000x

Graphene is an important material for sensing and energy storage applications. Since the vast majority of sensing and energy storage chemical and electrochemical systems require bulk quantities of graphene, thermally reduced graphene oxide (TRGO) is commonly employed instead of pristine graphene. The sp^2 planar structure of TRGO is heavily damaged, consisting of a very short sp^2 crystallite size of nanometre length and with areas of sp^3 hybridized carbon. Such a structure of TRGO is reminiscent of the key characteristic of the structure of amorphous carbon, which is defined as a material without long-range crystalline order consisting of both sp^2 and sp^3 hybridized carbons. Herein, we describe the characterization of TRGO, its parent graphite material and carbon black (a form of amorphous carbon) *via* transmission electron microscopy, Raman spectroscopy, X-ray photoelectron spectroscopy (XPS) and cyclic voltammetry experiments. We used the data obtained as well as consideration of practical factors to perform a comparative assessment of the relative electrochemical performances of TRGO against amorphous carbon. We found out that TRGO and amorphous carbon exhibit almost identical characteristics in terms of density of defects in the sp^2 lattice and a similar crystallite size as determined by Raman spectroscopy. These two materials also exhibit similar amounts of oxygen containing groups as determined by XPS and nearly indistinguishable cyclic voltammetric response providing almost identical heterogeneous electron transfer constants. This leads us to conclude that for some sensing and energy storage electrochemical applications, the use of amorphous carbon might be a much more economical solution than the one requiring digestion of highly crystalline graphite with strong oxidants to graphite oxide and then thermally exfoliating it to thermally reduced graphene oxide.

Introduction

There is significant interest in using graphene for electrochemical applications.[1] Graphene refers to a monoatomic thick allotrope of carbon, in which sp^2-hybridized carbon atoms are arranged in a planar honeycomb lattice structure.[2,3] As an isolated single layer carbon material, graphene exhibits many unique properties, particularly unprecedented intrinsic strength and Young's modulus values,[4] high specific surface area,[5] excellent electrical and thermal conductivity,[6,7] and a fast heterogeneous electron transfer (HET) rate at plane edges and defect sites.[7] Such characteristics make the use of graphene in electrochemical sensors highly advantageous; unfortunately, current methods available for the preparation of truly pristine graphene are still being optimized and are not yet scalable to production in bulk quantities, which is necessary for usage as electrode materials.[8] As a result, electrochemical studies on graphene and its practical applications have been largely limited to graphene analogues collectively known as "chemically modified graphenes" (CMGs) as suggested by Ruoff *et al.*[9] These materials possess functional groups covalently attached to the surface of individual sheets of graphitic carbon. One such class of CMGs are the reduced graphene oxides, carbon materials prepared from the reduction of graphite/graphene oxide *via* chemical, electrochemical, microwave or thermal means.[10] These reduced graphene oxide materials attempt to approach the nature of pristine graphene but often suffer from heteroatomic contamination and/or defects in the graphene plane, inevitably incorporated during the preparation process. Nevertheless, their use continues to be widespread due to their comparative ease of production as well as scalability.

The high-temperature thermal treatment of graphite oxide yields a highly expanded carbon material that has an appearance ranging from accordion/worm-like structures to a "fluffy" agglomerated powder, depending on the degree of exfoliation.[11,12] This expansion occurs due to interlayer pressure build-up from the evolution of gases, which was demonstrated to arise mainly from the decomposition of oxygen-containing groups

Division of Chemistry & Biological Chemistry, School of Physical and Mathematical Sciences, Nanyang Technological University, Singapore, 637371, Singapore. E-mail: pumera@ntu.edu.sg; Fax: +65 6791-1961

present, rather than the vaporization of intercalating species. The removal of oxygen-containing groups also leads to the simultaneous reduction of the material from its original state.[13] Such thermally exfoliated carbon materials can be generally termed as "thermally reduced graphene oxide" (TRGO) as a result. TRGO displays a high density of topographical defects as compared to pristine graphene due to the initial oxidation of the carbon backbone as well as the thermal shock treatment induced decomposition of oxygen-containing groups.[14] The introduction of holes and defects in the plane does come with certain advantages with regards to electrochemical sensing: TRGO usually exhibits far greater specific surface area and overall HET rates as compared to other forms of reduced graphene oxides.[15,16]

Amorphous carbon (AC) is yet another one of the many allotropes of carbon, broadly encompassing carbon materials without long-range crystalline order.[3] ACs as a whole can have any ratio of sp^3, sp^2 and even sp^1 sites; small homogeneous domains of these allow ACs to show some degree of short-range order, though the interbonding angles or interatomic distances are subject to deviations due to the presence of dangling bonds.[3,17] AC impurities are known to exist at significant levels in carbon nanotubes (CNTs) prepared using typical synthetic procedures,[18] and have been shown to dominate the electrochemical behaviour of electrodes modified with carbon materials containing AC impurities.[19] Carbon black is an example of AC which is industrially and commercially important, being heavily used in pigmenting and automobile tire reinforcing industries. The dominant production method, oil furnace process, accounts for >90% of all carbon black production in the U.S. and involves the partial combustion of aromatic liquid hydrocarbons in a furnace that ultimately leads to the collection of extremely fine black particles.[20] These particles consist of colloidal AC spheres and fused aggregates not exceeding 1000 nm in size as defined by IUPAC[3] and are usually highly pure (>90% elemental carbon) and arranged in an aciniform structure.[21]

It should be noted that due to the destruction of the crystalline sp^2 lattice during the preparation, TRGO exhibits quasi-amorphous character comprising small sp^2-bonded graphene islands separated by topological defects and holes,[14] thereby mirroring the abovementioned definition of AC. This description is also similar to what is observed by high resolution transmission electron microscopy of poorly graphitized carbon black, showing many small, separated pseudo-graphitic planes dispersed in an amorphous matrix.[22,23] It is thus plausible to suggest that despite their morphological differences, the two materials may not differ significantly in their electrochemical properties.

To the best of our knowledge, there is no comparative study to date on the relative electrochemical behaviours of TRGO and AC, which could provide valuable insight into the choice of such materials in the fabrication of electrosensing devices. This is particularly relevant when considering the steps necessary to obtain TRGO *versus* AC: TRGO is derived from the oxidation of powdered graphite *via* chemical methods followed by its subsequent thermal reduction, which is both time consuming and incurs additional costs. In contrast, AC in the form of carbon black is readily available, being produced in massive quantities (2006 worldwide production was 8.1 million metric tons)[21] and can be utilized as obtained from suppliers, as well as at low cost. In this work, we report on the direct comparison of TRGO and AC *via* materials characterization, including an assessment of their relative electrochemical performances using several redox probes.

Experimental section

Materials

Carbon black (Grade 5358R, 29 nm) was obtained from Asbury Carbons, USA. Graphite powder (<20 μm), fuming nitric acid (>90%), sulfuric acid (95–98%), potassium chlorate (98%), hydrochloric acid (37%), phosphate buffer powder, *N*,*N*-dimethylformamide, potassium hexacyanoferrate(III), L-ascorbic acid and hexaammineruthenium(III) chloride were purchased from Sigma-Aldrich, Singapore. Deagglomerated alpha alumina powder (0.05 μm) was purchased from Struers, Singapore. The glassy carbon (GC) working electrode, Ag/AgCl reference electrode, and Pt auxiliary electrode were obtained from CH Instruments, USA.

Apparatus

Transmission electron micrographs were obtained with a JEM 1400 transmission electron microscope (JEOL, Japan) operating at 120 kV. The sample for TEM was prepared by depositing 1 μL of the material suspension (1 mg mL^{-1}) onto a copper TEM grid and allowed to dry in air. Raman spectra were obtained with a confocal micro-Raman LabRam HR spectrometer (Horiba Scientific, Japan) with an excitation wavelength of 514.5 nm using an argon ion laser beam employing backscattering geometry with a CCD detector. The samples for X-ray photoelectron spectroscopy (XPS) were prepared by coating carbon tape with a uniform layer of the materials studied; XPS measurements were then carried out with a Phoibos 100 spectrometer (SPECS, Germany) with a monochromatic Mg X-ray source. Relative sensitivity factors were used for evaluation of C : O ratios from wide spectra XPS measurements. All voltammetric experiments were carried out on a μAutolab type III electrochemical analyzer (Eco Chemie, The Netherlands) connected to a personal computer and controlled by General Purpose Electrochemical Systems Version 4.9 software (Eco Chemie). Electrochemical experiments were carried out in a 20 mL electrochemical cell at room temperature with a three-electrode configuration, with Ag/AgCl as the reference electrode and Pt as the auxiliary electrode. All electrochemical potentials in this paper are stated *versus* Ag/AgCl reference electrode.

Procedures

GC electrode surfaces were renewed by polishing for 2 min with alumina slurry on a polishing pad and washed thoroughly with deionised water of resistivity not less than 18.2 MΩ cm obtained from an ion-exchange system Milli-Q (Millipore).

Suspensions of the carbon materials in DMF were prepared with a concentration of 1 mg mL^{-1} with 30 min sonication. Immobilization of the relevant carbon material on the GC electrode was carried out by depositing a 1 μL aliquot of the suspension onto the electrode surface and the solvent was evaporated under a lamp for 25 min to provide a modified electrode. Prior to each deposition, the suspensions were sonicated for an additional 5 min to ensure homogeneity.

Thermally reduced graphene oxide (TRGO) was prepared by following the methods in our previous study.[16]

Cyclic voltammetry experiments were performed at a scan rate of 100 mV s^{-1} with 50 mM phosphate buffer solution (pH 7.2) as the supporting electrolyte for potassium ferricyanide, ascorbic acid and hexaammineruthenium(III) chloride redox probes, with the number of measurements $n = 5$ for the purpose of reproducibility calculations (RSD values).

The crystallite size (L_a) of the sp^2 lattice was calculated using the equation:

$$L_a = 2.4 \times 10^{-10} \times \lambda_{laser}{}^4 \times I_G/I_D$$

where λ_{laser} is the wavelength of the laser in nm, I_G and I_D are intensities of the Raman G and D bands respectively.

k^0_{obs} values were calculated according to the Nicholson method[34] relating ΔE values to a dimensionless kinetic parameter ψ, leading to k^0_{obs} *via* the equation:

$$k^0 = \Psi \left[D_O \pi \nu \left(\frac{nF}{RT} \right)^{1/2} \right] \left(\frac{D_R}{D_O} \right)^{\alpha/2}$$

where D_O and D_R are the diffusion coefficients[35] for potassium ferricyanide and potassium ferrocyanide respectively at 298 K, n is the number of electrons transferred, F is the Faraday constant, R is the ideal gas constant, T is the temperature in K and α is the transfer coefficient (0.5).

Capacitance values were calculated using the equation:

$$C = \frac{dQ}{dt} = \frac{I}{\nu}$$

where C is the capacitance in F, I is the current in A and ν is the scan rate in V s^{-1}. Anodic current values were measured at a potential of +0.15 V for the purpose of these calculations.

Results and discussion

To simulate "true" amorphous carbon (where only short-range crystalline order exists), poorly graphitized carbon black was used in the proceeding experiments due to its low grade of crystallinity.[19] Graphite was used throughout the course of this work for comparison purposes as a reference material representing also the starting component used to produce the TRGO. Transmission electron microscopy was firstly used to visualize the morphological differences between graphite, carbon black and TRGO. It can be seen in Fig. 1 that graphite exhibits a typical multi-layered structure with sharp edges and smooth basal planes. The carbon black sample presented the aggregate aciniform structure with colloidal spherical units of about 30 nm in diameter. TRGO shows the single–few layer sheet morphology with several wrinkles on the surface as generally observed after thermal treatments. Such wrinkles are due to the presence of sp^3 hybridized carbons within the graphene network which cause structure distortions. Due to such a difference in morphology, the three materials presented different surface areas of 9, 79 and 563 m^2 g^{-1}, for graphite, carbon black and TRGO, respectively, measured using the BET method. Despite the morphological differences, structural and surface chemical similarities are expected for TRGO and carbon black. Samples of TRGO (prepared in-house as described in the Experimental section) and carbon black (used here as surrogate of AC) were then characterized using Raman spectroscopy and X-ray photoelectron spectroscopy (XPS) to investigate their defect density and amount of oxygen-containing groups, both of which are well known to affect the electrochemistry of many compounds.[24]

The Raman spectra of the materials investigated are shown in Fig. 2. Features of primary significance in the spectra are the G-band at ~1575 cm^{-1} representing the sp^2 lattice, and the D-band at ~1350 cm^{-1} related to defects in the sp^2 lattice structure. For ease of visual comparison, the signals were normalized according to the G-band intensity. The spectrum of the parent graphite also displays a strong 2D-signal at ~2720 cm^{-1} known to occur in multilayer graphene structures[25] which is visibly different or lacking in the spectra of both AC and TRGO, indicating the presence of significant structural defects.

Using the peak signal intensities, D/G ratios of the materials were calculated as follows: graphite, 0.08; AC, 0.91; TRGO, 1.04. The parent graphite exhibits as expected by far the most ordered sp^2 structure, while AC and TRGO gave values that displayed high density of defects. This is expected for TRGO due to the thermal shock exfoliation process used for its preparation from graphite oxide, introducing even more defects into the sp^2 plane that was already heavily disrupted due to the oxidation step.[26]

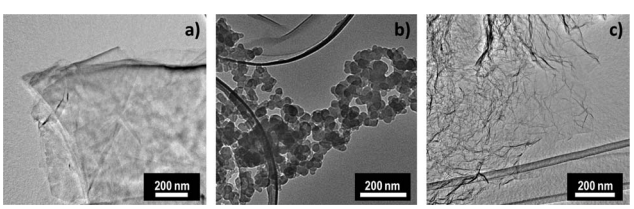

Fig. 1 Transmission electron micrographs of (a) graphite, (b) carbon black and (c) TRGO.

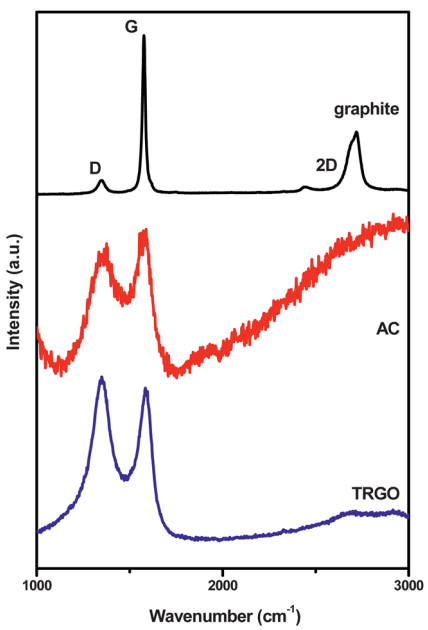

Fig. 2 Raman spectra of graphite, amorphous carbon (AC) and TRGO normalized to G-band intensity.

Since the manufacturing process of furnace carbon black involves high temperature (>1000 °C) partial combustion of hydrocarbons, it could conceivably introduce defects in the sp^2 plane in a similar manner to TRGO (being also exfoliated at temperatures >1000 °C). The broader bands (as compared to graphite) present in the AC and TRGO spectra also indicate small crystallite sizes (L_a) due to the introduction of disorder into the base graphite structure.[27] L_a values for graphite, AC and TRGO were found to be 198, 18 and 16 nm, respectively, as derived from the Raman spectra.

XPS techniques are able to determine the elemental composition as well as chemical and electronic states of elements on the surface of a material. The surface chemistry of modified electrodes is known to regularly influence electrochemical processes in a number of ways, for example adsorption/chelation effects arising from surface charge, which alter the heterogeneous electron transfer (HET) rates.[28–30] For the three carbon materials, the influence manifests itself primarily in the form of oxygen-containing groups, which makes XPS useful for investigating this phenomenon. Fig. 3 shows XPS wide spectra for graphite, AC and TRGO. Using the C1s and O1s signal intensities, C : O ratios for the materials were calculated and were found to be 43.4, 10.1 and 16.0 for graphite, AC and TRGO, respectively. Voltammetric characterization was carried out *via* cyclic voltammetry experiments using a selection of three commonly employed redox probes: $[Fe(CN)_6]^{4-/3-}$, ascorbic acid, and $[Ru(NH_3)_6]^{2+/3+}$. Fig. 4 shows cyclic voltammograms (CVs) recorded for graphite, AC and TRGO modified GC electrodes in 10 mM ferro/ferricyanide using 50 mM phosphate buffer solution (PBS) as the background electrolyte.

Extensive studies have shown that the electron transfer of the ferro/ferricyanide redox probe occurs through an inner-sphere mechanism showing considerable sensitivity to the electrode surface, with a small amount of perturbation arising from the repulsive interaction between negatively charged ferricyanide complexes and oxygen-containing groups.[24] Peak-to-peak separation (ΔE) values are inversely related to the rate of HET; smaller ΔE values correspond to faster HET which generally indicates better performance with regards to electrochemical sensors.

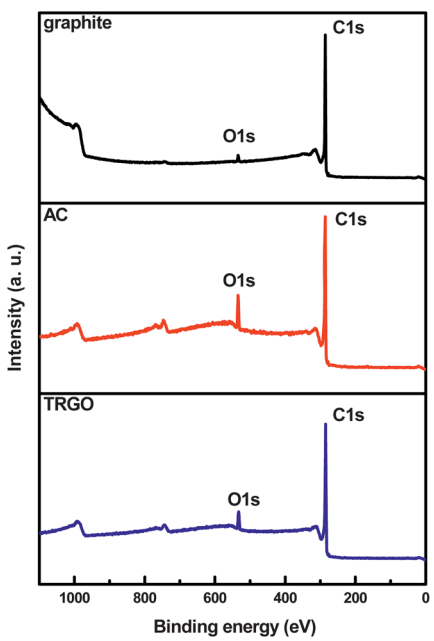

Fig. 3 XPS wide spectra for graphite, amorphous carbon (AC) and TRGO showing relative C : O peak intensities.

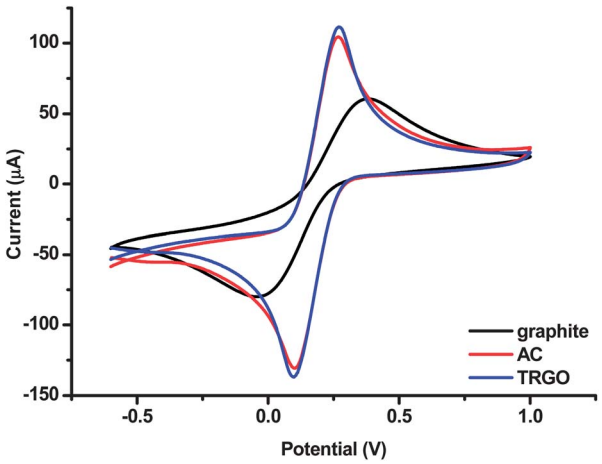

Fig. 4 Cyclic voltammograms for 10 mM ferro/ferricyanide on graphite, amorphous carbon (AC) and TRGO modified GC electrodes. *Conditions*: scan rate, 100 mV s^{-1}; background electrolyte, 50 mM phosphate buffer solution (pH 7.4); reference electrode, Ag/AgCl.

The graphite modified electrode displayed the largest ΔE of 396 mV (RSD 10%) and the slowest HET of 7.52×10^{-5} cm s^{-1} (k^0_{obs}), while the AC and TRGO modified electrodes were virtually overlays of each other, having ΔE values of 166 mV (RSD 2%, $k^0_{obs} = 1.71 \times 10^{-3}$ cm s^{-1}) and 165 mV (RSD 3%, $k^0_{obs} = 1.74 \times 10^{-3}$ cm s^{-1}), respectively. The closeness of ΔE and HET constant values for these two materials is in agreement with their similar defect densities, and it appears that their relatively more different C : O ratios did not alter ΔE values to any significant extent.

Subsequent experiments were performed with the ascorbic acid (AA) probe, a biologically important organic compound vital in human nutrition that has antioxidant properties in the body. The electrochemical oxidation of ascorbic acid is known to be strongly sensitive to a variety of factors such as surface charge, density of edge/defect sites, electrode surface area as well as any oxygen containing groups present on the electrode surface. The results are shown in Fig. 5. As can be seen from the CVs, oxidation of AA occurred on the graphite modified electrode at +419 mV (RSD 5%), once again significantly higher than the other two materials. Interestingly, the TRGO modified electrode showed slightly better performance than the AC modified electrode, with oxidation of AA first occurring at +19 mV (RSD 13%) for the former and +38 mV (RSD 9%) for the latter. This may possibly be attributed to the lower amount of oxygen-containing groups in TRGO as compared to AC; it has been demonstrated that the introduction of oxygen-containing groups adversely affects HET rates at the electrode surface for the AA probe.[31] Both AC and TRGO modified electrodes also displayed a second oxidation peak at approximately +220 mV, which may indicate that these materials have heterogeneous surfaces (mixture of edge and basal planes) or it could arise from

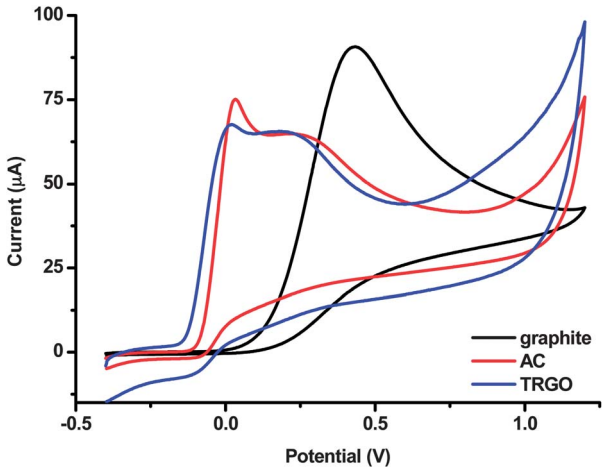

Fig. 5 Cyclic voltammograms for 5 mM ascorbic acid on graphite, amorphous carbon (AC) and TRGO modified GC electrodes. *Conditions*: scan rate, 100 mV s^{-1}; background electrolyte, 50 mM phosphate buffer solution (pH 7.4); reference electrode, Ag/AgCl.

a possible incomplete coverage/uneven distribution of these materials on the GC electrode surface. Additionally, it is worth noting that the occurrence of multiple oxidation signals is not present in reduced graphene oxides derived from chemical and electrochemical means,[16] hinting that thermal reduction of graphene oxide yields a material more resembling amorphous carbon than its chemically or electrochemically reduced analogues.

The final redox probe used to assess the electrochemical behaviour of modified electrodes was hexaammineruthenium(III) chloride. This redox system is highly insensitive to electrode surface modification owing to its outer-sphere electron transfer mechanism that does not involve specific adsorption to surface oxygen-containing groups.[32] The CVs for this probe are depicted in Fig. 6.

Unsurprisingly, all three carbon materials gave highly similar ΔE values (~70 mV) as a result of the probe's non-dependence on surface characteristics. The graphite modified electrode showed

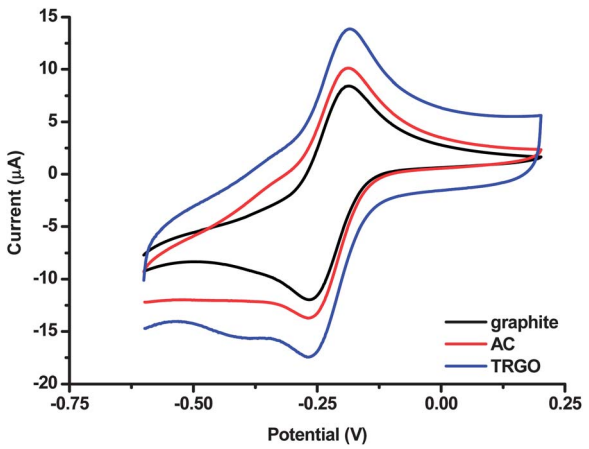

Fig. 6 Cyclic voltammograms for 1 mM hexaammineruthenium(III) chloride on graphite, amorphous carbon (AC) and TRGO modified GC electrodes. *Conditions*: scan rate, 100 mV s^{-1}; background electrolyte, 50 mM phosphate buffer solution (pH 7.4); reference electrode, Ag/AgCl.

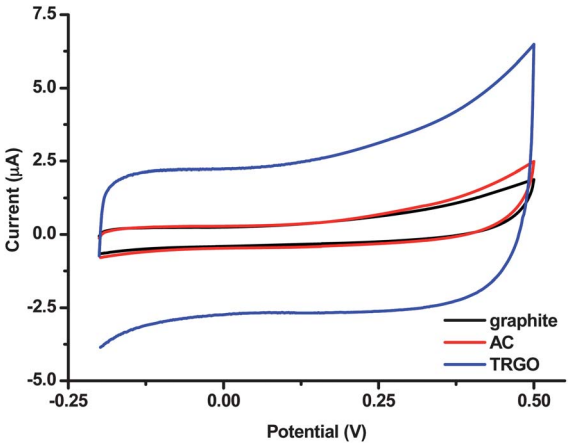

Fig. 7 Cyclic voltammograms for blank buffer solution on graphite, amorphous carbon (AC) and TRGO modified GC electrode. *Conditions*: scan rate, 100 mV s^{-1}; background electrolyte, 50 mM phosphate buffer solution (pH 7.4); reference electrode, Ag/AgCl.

an average ΔE of 70 mV (RSD 4%), as did AC (ΔE = 70 mV, RSD 1%). The TRGO modified electrode gave an insignificantly higher ΔE of 72 mV (RSD 3%). The most obvious difference in the CVs was the large increase in peak current values, which was due to the vastly differing capacitances of the three materials. This effect was investigated further as shown in Fig. 7, in which CVs were recorded for the modified electrodes in blank phosphate buffer solution.

It is clear that the capacitance of TRGO is vastly higher than that of graphite or AC; as can be seen from the CVs in Fig. 7, AC has a capacitance very similar to graphite in the scanned potential range. Weight specific capacitance (C_w) of graphite was found to be the lowest at 3.23 F g^{-1}, while AC gave a slightly higher value of 4.20 F g^{-1}. In contrast, C_w of TRGO was calculated to be 26.75 F g^{-1}, consistent with previous data obtained.[33] This makes TRGO suitable as a material for high energy supercapacitors which need to provide large power density within a short time frame. However, this may be undesirable in electrochemical sensing, especially in the determination of currents arising due to Faradaic processes occurring at the electrode surface.

Conclusion

In this study we have characterized AC and TRGO materials both physically (*via* transmission electron microscopy, Raman spectroscopy and XPS measurements) and electrochemically (through cyclic voltammetry experiments). We have demonstrated that despite noticeable differences in their morphologies, the oxygen content as well as the density of sp^2 plane defects of the two materials are equivalent giving rise to extremely similar electrochemical performance based on the three redox probes assessed here. Both AC and TRGO modified electrodes offered enhanced electrochemical performance over the electrode modified with the control parent graphite material. Utilizing TRGO as a sensing material did not have a perceivable advantage over AC for inner-sphere redox probes (*e.g.* $[Fe(CN)_6]^{4-/3-}$) as well as outer-sphere redox probes generally insensitive to surface oxygen-containing groups (*e.g.* $[Ru(NH_3)_6]^{2+/3+}$), while

only a slight decrease in oxidation potential was observed for the ascorbic acid probe. With regard to capacitance, the usage of TRGO is beneficial if this property is desired (for example in carbon-based supercapacitors), exhibiting sixfold to eightfold the weight specific capacitance of AC and graphite. However, for electrochemical sensing purposes we suggest AC as an electrode material *in lieu* of TRGO due to its low cost and time saving since it can be used "as is" from commercial suppliers, with little or no loss in electrochemical performance.

Acknowledgements

We wish to acknowledge NAP start-up grant (NTU) for financial support. We also wish to acknowledge the funding support for this project from Nanyang Technological University under the Undergraduate Research Experience on CAmpus (URECA) programme.

References

1 M. Pumera, *Chem. Soc. Rev.*, 2010, **39**, 4146–4157.
2 A. K. Geim and K. S. Novoselov, *Nat. Mater.*, 2007, **6**, 183191.
3 IUPAC, in *Compendium of Chemical Terminology, (the "Gold Book")*, ed. A. D. McNaught and A. Wilkinson, Blackwell Scientific Publications, Oxford, 2nd edn, 1997.
4 C. Lee, X. Wei, J. W. Kysar and J. Hone, *Science*, 2008, **321**, 385–388.
5 M. D. Stoller, S. Park, Y. Zhu, J. An and R. S. Ruoff, *Nano Lett.*, 2008, **8**, 3498–3502.
6 A. A. Balandin, S. Ghosh, W. Z. Bao, I. Calizo, D. Teweldebrhan, F. Miao and C. N. Lau, *Nano Lett.*, 2008, **8**, 902–907.
7 W. Cai, Y. Zhu, X. Li, R. D. Piner and R. S. Ruoff, *Appl. Phys. Lett.*, 2009, **95**, 123115.
8 M. Pumera, *Chem. Rec.*, 2009, **9**, 211–223.
9 D. R. Dreyer, R. S. Ruoff and C. W. Bielawski, *Angew. Chem., Int. Ed.*, 2010, **49**, 9336–9344.
10 D. R. Dreyer, S. Park, C. W. Bielawski and R. S. Ruoff, *Chem. Soc. Rev.*, 2010, **39**, 228–240.
11 A. Celzard, J. F. Mareche and G. Furdin, *Prog. Mater. Sci.*, 2004, **50**, 93–179.
12 S. R. C. Vivekchand, C. S. Rout, K. S. Subrahmanyam, A. Govindaraj and C. N. R. Rao, *J. Chem. Sci.*, 2008, **120**, 9–13.
13 M. J. McAllister, J. L. Li, D. H. Adamson, H. C. Schniepp, A. A. Abdala, J. Liu, M. Herrera-Alonso, D. L. Milius, R. Car, R. K. Prud'homme and I. A. Aksay, *Chem. Mater.*, 2007, **19**, 4396–4404.
14 C. Gomez-Navarro, J. C. Meyer, R. S. Sundaram, A. Chuvilin, S. Kurasch, M. Burghard, K. Kern and U. Kaiser, *Nano Lett.*, 2010, **10**, 1144–1148.
15 Y. Zhu, S. Murali, W. Cai, X. Li, J. W. Suk, J. R. Potts and R. S. Ruoff, *Adv. Mater.*, 2010, **22**, 3906–3924.
16 A. Ambrosi, A. Bonanni, Z. Sofer, J. S. Cross and M. Pumera, *Chem.–Eur. J.*, 2011, **17**, 10763–10770.
17 A. C. Ferrari and J. Robertson, *Phys. Rev. B: Condens. Matter Mater. Phys.*, 2000, **61**, 14095–14107.
18 K. B. Shelimov, R. O. Esenaliev, A. G. Rinzler, C. B. Huffman and R. E. Smalley, *Chem. Phys. Lett.*, 1998, **282**, 429–434.
19 A. Ambrosi and M. Pumera, *J. Phys. Chem. C*, 2011, **115**, 25281–25284.
20 R. W. Serth and T. W. Hughes, *Source Assessment: Carbon Black Manufacture*, U.S. Environmental Protection Agency, Cincinnati, OH, 1977.
21 International Carbon Black Association, *Carbon Black User's Guide*, 2004.
22 N. Larouche and B. L. Stansfield, *Carbon*, 2010, **48**, 620–629.
23 P. Xue, J. Gao, Y. Bao, J. Wang, Q. Li and C. Wu, *Carbon*, 2011, **49**, 3346–3355.
24 X. B. Ji, C. E. Banks, A. Crossley and R. G. Compton, *ChemPhysChem*, 2006, **7**, 1337–1344.
25 A. C. Ferrari, *Solid State Commun.*, 2007, **143**, 47–57.
26 H. C. Schniepp, J. L. Li, M. J. McAllister, H. Sai, M. Herrera-Alonso, D. H. Adamson, R. K. Prud'homme, R. Car, D. A. Saville and I. A. Aksay, *J. Phys. Chem. B*, 2006, **110**, 8535–8539.
27 T. Jawhari, A. Roid and J. Casado, *Carbon*, 1995, **33**, 1561–1565.
28 A. F. Holloway, G. G. Wildgoose, R. G. Compton, L. D. Shao and M. L. H. Green, *J. Solid State Electrochem.*, 2008, **12**, 1337–1348.
29 M. Osawa, M. Tsushima, H. Mogami, G. Samjeské and A. Yamakata, *J. Phys. Chem. C*, 2008, **112**, 4248–4256.
30 R. L. McCreery, *Chem. Rev.*, 2008, **108**, 2646–2687.
31 J. G. S. Moo, A. Ambrosi, A. Bonanni and M. Pumera, *Chem.–Asian J.*, 2012, **7**, 759–770.
32 P. H. Chen and R. L. McCreery, *Anal. Chem.*, 1996, **68**, 3958–3965.
33 L. Buglione, E. L. K. Chng, A. Ambrosi, Z. Sofer and M. Pumera, *Electrochem. Commun.*, 2012, **14**, 5–8.
34 R. S. Nicholson, *Anal. Chem.*, 1965, **37**, 1351–1355.
35 R. N. Adams, in *Electrochemistry at Solid Electrodes*, Marcel-Dekker, New York, 1969.